Silicene spintronics: Fe(111)/silicene system for efficient spin injection

Jiaqi Zhou,[1,2,3] Arnaud Bournel,[3] Yin Wang,[4] Xiaoyang Lin,[1,2] Yue Zhang,[1,2] and Weisheng Zhao[1,2,a)]

[1]*Fert Beijing Research Institute, Beihang University, BDBC, Beijing 100191, China*
[2]*School of Electronic and Information Engineering, Beihang University, Beijing 100191, China*
[3]*Centre de Nanoscience et de Nanotechnologies, Univ. Paris-Sud, Univ. Paris-Saclay, CNRS, F-91405 Orsay, France*
[4]*Department of Physics and the Center of Theoretical and Computational Physics, The University of Hong Kong, Hong Kong, China*

(Received 6 August 2017; accepted 24 October 2017; published online 2 November 2017)

Silicene is an emerging 2D material with advantages of high carrier mobility, compatibility with the silicon-based semiconductor industry, and the tunable gap by a vertical electrical field due to the buckling structure. In this work, we report a first-principles investigation on the spin injection system, which consists of a Fe(111)/silicene stack as the spin injector and pure silicene as the spin channel. An extremely high spin injection efficiency (SIE) close to 100% is achieved. The partial density of states of Fe layers in the Fe(111)/silicene stack shows that spin-down states dominate above the Fermi level, resulting in a negligible spin-up current and high SIE. The transmission spectra have been investigated to analyze the spin-resolved properties. The spin injection system based on silicene is promising for the efficient silicon-based spintronics devices such as switching transistors. *Published by AIP Publishing*. https://doi.org/10.1063/1.4999202

Spintronics utilizes the spin degree of freedom of electrons to construct information storage and process devices, such as the spin logic circuit.[1] To achieve spin logic devices with merits of high-reliability and low-power operation, it is necessary to develop a system with a high spin injection efficiency (SIE) and excellent spin-transport properties.[2] Due to the exceptional characters of low dimension, massless Dirac fermion, and weak spin-orbit coupling (SOC),[3,4] graphene has been widely investigated as the spin transport channel.[5–10] Meanwhile, silicene, the monolayer of silicon with high Fermi velocity and mobility, has attracted increasing interest,[11–17] and many successful synthesis works have been reported recently.[18–21] Superior to graphene, silicene overcomes the problem of compatibility with the present silicon-based semiconductor technology, which is critical for the practical application of spin logic devices.[13] Besides, it has been reported that the tunable gap can be opened in silicene by applying a vertical electrical field thanks to the buckling structure.[22] This character has significant meaning for the switching transistors and logic devices. Note that the SOC of silicene is 1.55 meV, higher than that of graphene but much lower than that of Cu and Ag, which are common materials as spin transport channels for low-power spintronic devices.[23,24] As a result, silicene is a good candidate for spin channels. Here, we propose a spin injection system based on the Fe(111)/silicene stack and silicene channel and report a remarkable spin injection efficiency.

In this work, we present a non-equilibrium first-principles study on the spin injection system based on the Fe(111)/silicene structure. The atomic structure of the spin injection system is shown in Fig. 1. It is known that Fe is one of the most common metals used in the ferromagnetic device.[25] The whole transport system consists of the Fe(111)/silicene (FS) stack and pure silicene channel, where the former (latter) acts as the left (right) lead, and both leads are semi-infinite. Experimental work has reported that silicene can be transferred by the encapsulation method, so we assume that silicene is transferred on Fe layers while keeping the silicene structure.[20,26] The surface condition matters greatly in density functional theory (DFT) calculation.[27] For the primitive cell FS stack, the Si atom at a high position is at the top of the second Fe atom layer, while the low-position Si atom locates exactly above the third Fe atom layer. This configuration, with 1.1 Å interlayer space between silicene and the top Fe layer, as well as the closest Si-Fe distance of 2.48 Å, has been demonstrated as the most stable structure by the surface separation test with $33 \times 33 \times 1$ **k**-mesh in VASP.[28,29] The spin transport is along the x direction, and the scattering

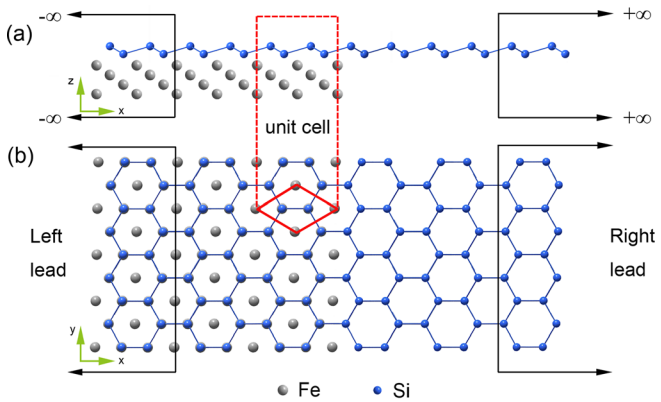

FIG. 1. Diagram of the spin injection system. The silicene monolayer is on the Fe(111) layers. The black arrows indicate the left and right leads, extending to $\pm\infty$, which consist of the Fe(111)/silicene stack (left lead) as the spin injector and pure silicene (right lead) as the spin transport channel. (a) The side view. (b) The top view. The red box indicates the unit cell of the Fe(111)/silicene stack.

a)Author to whom correspondence should be addressed: weisheng.zhao@buaa.edu.cn

region along the transport direction is 26.74 Å. The system extends periodically in the y direction, and the normal direction of the silicene plane is the z direction where the vacuum layer exists. The unit cell is shown in the red box, and the lattice constant is kept to be 3.86 Å. Note that the lattice constant of bcc Fe is 2.86 Å, silicene has the lattice constant of 3.86 Å, and the buckling distance was 0.46 Å.[22,23] For the sake of Fe(111)/silicene match, Fe is homogeneously strained by less than 5%, which makes negligible influence on the band structure.

We employed the first-principles transport package NanoDCAL[30,31] to compute the spin-dependent transport properties of the system. This package combines DFT with the Keldysh Non-Equilibrium Green's Function (NEGF) formalism. In the NEGF-DFT transport simulation, the physical quantities are expanded by a linear combination of atomic orbital (LCAO) basis sets at the double-zeta plus polarization orbital (DZP) level. The spin-dependent current I_σ, where σ indicates the spin-up or spin-down state, is obtained as follows:

$$I_\sigma = \frac{e}{h}\int_{-\infty}^{+\infty} T_\sigma(E,V)[f_L(E,\mu_L) - f_R(E,\mu_R)]dE, \qquad (1)$$

where e, h, and T_σ are the electron charge, Plank's constant, and the transmission coefficient, respectively. f_L and f_R in the equation are the Fermi distribution functions of the left and right leads, respectively. Under the voltage bias V, the chemical potentials of the left lead (right lead) is shifted to $\mu_L = E_F - eV/2$ ($\mu_R = E_F + eV/2$), where E_F is the Fermi level. A $1 \times 21 \times 1$ k-point mesh was used for the self-consistent calculation of the device, and a much denser sampling of $1 \times 500 \times 1$ was employed for transmission property calculation.

Figure 2 presents the calculated spin-resolved currents and total currents, as well as the SIE of the whole system. The SIE is defined as

$$SIE = \left|\frac{I_{up} - I_{down}}{I_{up} + I_{down}}\right| \times 100\%, \qquad (2)$$

where I_{up} is the spin-up current and I_{down} is the spin-down current. In Fig. 2(a), it can be found that the spin-down current is remarkably higher than the spin-up current at finite positive bias voltage, and the spin-down current rises prominently with the increasing bias, while the spin-up current remains low, until the bias reaches up to 60 mV. For the negative bias, the condition is opposite and spin-up current is higher than spin-down current. Figure 2(b) presents high SIE at various biases. Due to the zero-current, SIE cannot be defined at zero bias voltage, so this point is excluded. For the positive bias, SIE is close to 100% from 10 mV to 50 mV and declines from 60 mV. For the negative bias, SIE reaches up to the 78% peak at −10 mV and then decreases with the increasing bias.

To understand the remarkable SIE, we investigated the projected band structure and the partial density of states (PDOS). Figure 3(a) shows the spin-up band, and Fig. 3(b) presents the spin-down band. The black up-triangles (blue down-triangles) show the 2p character of the high-position (low-position) Si atom, and the red dots represent the 3d character of Fe atoms. It can be observed that the Dirac cone of silicene disappears due to the influence of Fe layers, and Fe 3d character bands cross the E_F and K point, while K is the Dirac point in the pure silicene band. Figure 3(c) presents the PDOS of all Fe atoms in the FS stack. It should be noticed that there is almost no spin-up state above E_F. Consequently, the spin-down state contributes primarily to the current, and the d_z^2 orbit is prominent shown as the red line. This leads to high spin-down current and high SIE in the FS-silicene channel transport system. Below E_F, spin-up states occupy the leading position but not overwhelming, which explains that for the negative bias, spin-up current dominates, while the SIE is not relatively high.

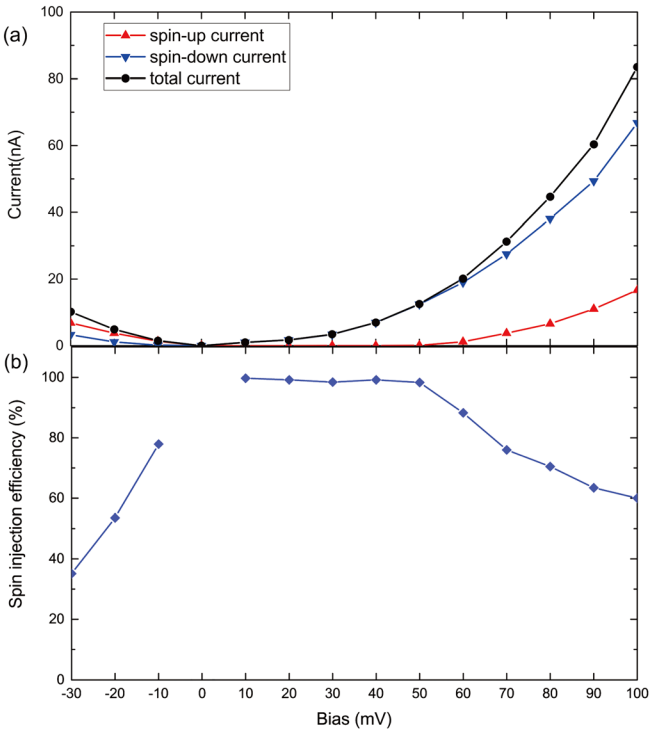

FIG. 2. Spin-resolved currents, the total current, and the spin injection efficiency of the whole system. (a) Spin-resolved currents and the total current. (b) Spin injection efficiency, which reaches up to nearly 100% between 10 mV and 50 mV bias.

The transmission spectrum $T(E,V)$ at a finite bias for the whole system is shown in Fig. 4. The current is obtained by integrating the transmission probability over the bias window $-V/2 \le E \le +V/2$, and the bias window is shown as the green dashed line. In Fig. 4(a), for 30 mV bias, the bias window nearly locates within the transmission gap for the spin-up condition, resulting in a dominant spin-down transport and nearly 100% SIE, as shown in Fig. 2. In Fig. 4(b), for 60 mV bias, spin-down transmission strengthens with the increasing bias, while spin-up transmission is still suppressed by a transmission gap. In Fig. 4(c), for the 90 mV bias, the spin-up transmission moves into the bias window and narrows the difference between the spin-up current and spin-down current. As a result, there is a decline in SIE, as shown in Fig. 2(b). The transmission spectra correspond well to the spin-resolved IV curves and further explain high SIEs.

In summary, we theoretically investigated the spin transport in the silicene channel with the Fe(111)/silicene stack

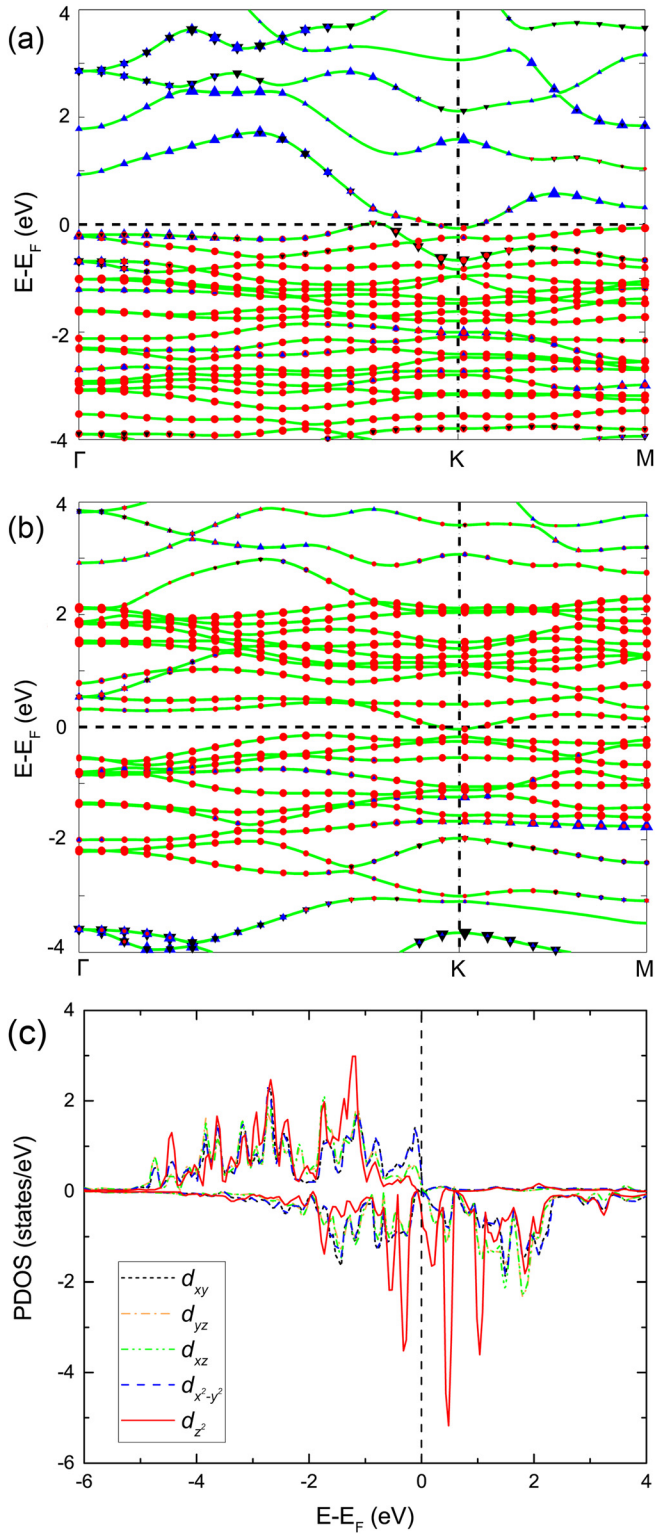

FIG. 3. Band structure of the Fe(111)/silicene primitive cell stack for the (a) spin-up condition and (b) spin-down condition. E_F is indicated by the horizontal dashed line, while the K point is indicated by the vertical dashed lines. The black up-triangles (blue down-triangles) show the 2*p* character of the high-position (low-position) Si atom, and the red dots represent the 3*d* character of Fe atoms. (c) Partial density of states (PDOS) of Fe atoms in the Fe(111)/silicene stack.

injector. Our non-equilibrium first-principles transport calculations illustrate that this spin injection system exhibits high SIEs close to 100%, which originate from the unique PDOS of Fe atoms in the Fe(111)/silicene stack. Only spin-down

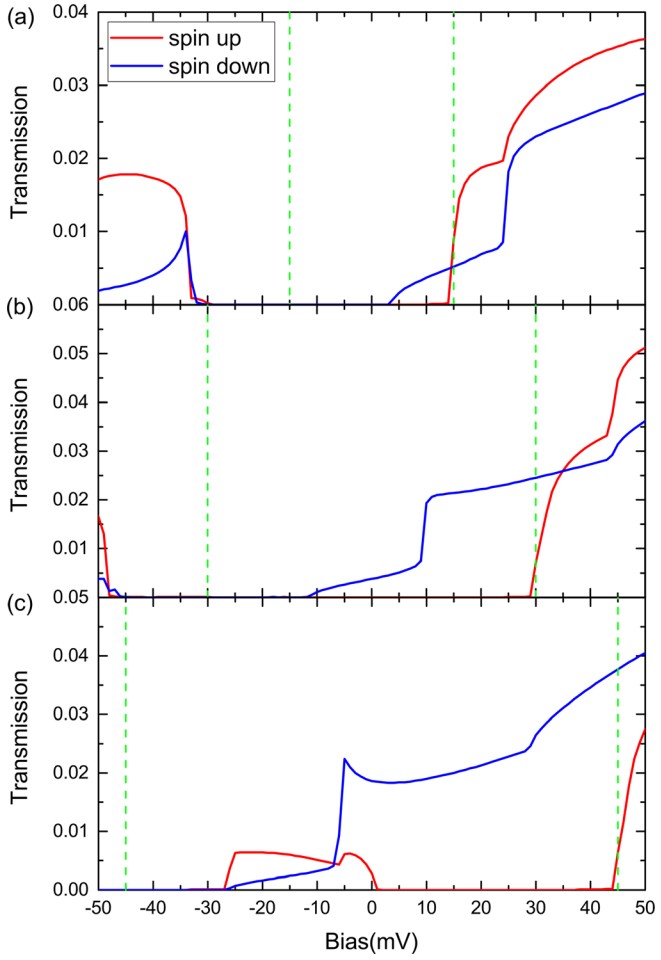

FIG. 4. Transmission coefficients versus electron energy for the whole system at different bias voltages V: (a) $V = 30$ mV, (b) $V = 60$ mV, and (c) $V = 90$ mV. The bias window is between the two green dashed lines, and the zero energy point is set at the middle of the bias window.

states exist above E_F, which leads to an overwhelming spin-down current and high SIE. The energy-resolved transmission spectra are investigated to understand the spin-resolved current and high SIEs. This work presents the Fe(111)/silicene structure as a good candidate for achieving efficient spin injection devices, while silicene is an ideal spin channel with prominent characters, such as tunable gap by the field and compatibility with the silicon-based semiconductor industry. This work would benefit the design of silicene devices and boost the development of silicene spintronics.

The authors would like to acknowledge the support by the projects from the National Natural Science Foundation of China (Nos. 61571023, 61501013, 51602013, and 61627813), the Beijing Municipal of Science and Technology (No. D15110300320000), the International Collaboration Project from the Ministry of Science and Technology in China (No. 2015DFE12880), Beijing Natural Science Foundation (No. 4162039), and the 111 project in China (No. B16001). Jiaqi Zhou acknowledges the support from the China Scholarship Council (CSC) program.

[1]A. D. Kent and D. C. Worledge, Nat. Nanotechnol. **10**, 187 (2015).
[2]J. A. Currivan-Incorvia, S. Siddiqui, S. Dutta, E. R. Evarts, J. Zhang, D. Bono, C. A. Ross, and M. A. Baldo, Nat. Commun. **7**, 10275 (2016).

[3]A. K. Geim and K. S. Novoselov, Nat. Mater. **6**, 183 (2007).
[4]A. Avsar, J. Y. Tan, T. Taychatanapat, J. Balakrishnan, G. K. W. Koon, Y. Yeo, J. Lahiri, A. Carvalho, A. S. Rodin, E. C. T. O'Farrell, G. Eda, A. H. Castro Neto, and B. Özyilmaz, Nat. Commun. **5**, 4875 (2014).
[5]W. Han, R. K. Kawakami, M. Gmitra, and J. Fabian, Nat. Nanotechnol. **9**, 794 (2014).
[6]J. Maassen, W. Ji, and H. Guo, Nano Lett. **11**, 151 (2011).
[7]Q. Wu, L. Shen, Z. Bai, M. Zeng, M. Yang, Z. Huang, and Y. P. Feng, Phys. Rev. Appl. **2**, 044008 (2014).
[8]S. Singh, J. Katoch, J. Xu, C. Tan, T. Zhu, W. Amamou, J. Hone, and R. Kawakami, Appl. Phys. Lett. **109**, 122411 (2016).
[9]Y. K. Luo, J. Xu, T. Zhu, G. Wu, E. J. McCormick, W. Zhan, M. R. Neupane, and R. K. Kawakami, Nano Lett. **17**, 3877 (2017).
[10]X. Lin, L. Su, Y. Zhang, A. Bournel, Y. Zhang, J.-O. Klein, A. Fert, and W. Zhao, Phys. Rev. Appl. **8**, 034006 (2017).
[11]S. Cahangirov, M. Topsakal, E. Akturk, H. Sahin, and S. Ciraci, Phys. Rev. Lett. **102**, 236804 (2009).
[12]B. Bishnoi and B. Ghosh, RSC Adv. **3**, 26153 (2013).
[13]J. Zhao, H. Liu, Z. Yu, R. Quhe, S. Zhou, Y. Wang, C. C. Liu, H. Zhong, N. Han, J. Lu, Y. Yao, and K. Wu, Prog. Mater. Sci. **83**, 24 (2016).
[14]A. Debernardi and L. Marchetti, Phys. Rev. B **93**, 245426 (2016).
[15]S. Trivedi, A. Srivastava, and R. Kurchania, J. Comput. Theor. Nanosci. **11**, 781 (2014).
[16]H. Da, W. Ding, and X. Yan, Appl. Phys. Lett. **110**, 141105 (2017).
[17]A. Ahmadi Fouladi, Physica E **91**, 101 (2017).
[18]P. Vogt, P. De Padova, C. Quaresima, J. Avila, E. Frantzeskakis, M. C. Asensio, A. Resta, B. Ealet, and G. Le Lay, Phys. Rev. Lett. **108**, 155501 (2012).
[19]L. Meng, Y. Wang, L. Zhang, S. Du, R. Wu, L. Li, Y. Zhang, G. Li, H. Zhou, W. A. Hofer, and H. J. Gao, Nano Lett. **13**, 685 (2013).
[20]L. Tao, E. Cinquanta, D. Chiappe, C. Grazianetti, M. Fanciulli, M. Dubey, A. Molle, and D. Akinwande, Nat. Nanotechnol. **10**, 227 (2015).
[21]L. Huang, Y. Zhang, Y. Zhang, W. Xu, Y. Que, E. Li, J. Pan, Y. Wang, Y. Liu, S. Du, S. Pantelides, and H. Gao, Nano Lett. **17**, 1161 (2017).
[22]Z. Ni, Q. Liu, K. Tang, J. Zheng, J. Zhou, R. Qin, Z. Gao, D. Yu, and J. Lu, Nano Lett. **12**, 113 (2012).
[23]C. Liu, W. Feng, and Y. Yao, Phys. Rev. Lett. **107**, 076802 (2011).
[24]H. Eckardt, L. Fritsche, and J. Noffke, J. Phys. F: Met. Phys. **14**, 97 (1984).
[25]E. M. Smelova, K. M. Tsysar, and A. M. Saletsky, Phys. Chem. Chem. Phys. **16**, 8360 (2014).
[26]K. S. Novoselov, A. Mishchenko, A. Carvalho, and A. H. Castro Neto, Science **353**, aac9439 (2016).
[27]O. O. Brovko, V. Stepanyuk, and P. Bruno, Phys. Rev. B **78**, 165413 (2008).
[28]G. Kresse and J. Hafner, Phys. Rev. B **48**, 13115 (1993).
[29]G. Kresse and J. Furthmüller, Phys. Rev. B **54**, 11169 (1996).
[30]J. Taylor, H. Guo, and J. Wang, Phys. Rev. B **63**, 121104(R) (2001).
[31]J. Taylor, H. Guo, and J. Wang, Phys. Rev. B **63**, 245407 (2001).